## II. THE EXPERIMENTS

Cross sections for inelastic e-p and e-d scattering were measured over a range of scattering angles in two separate experiments that employed similar experimental apparatus and data analysis methods. Electrons of fixed primary energy scattered from liquid hydrogen and deuterium targets and were momentum-analyzed in a focusing spectrometer set at fixed scattering angles. A number of momentum spectra, each covering a range of E' for fixed values of E, were measured at each angle to permit model-independent radiative corrections to be made.

In experiment A[24], cross sections were measured with the SLAC 8 GeV spectrometer at scattering angles of 18, 26, and 34 degrees for primary energies ranging from 4.5 GeV to 18.0 GeV and scattered energies ranging from 1.0 GeV to 8.75 GeV, as shown in Figure (2). Earlier inelastic e-p cross section measurements were repeated with improved accuracies. Inelastic e-p and e-d cross sections were measured alternately over the entire kinematic range. Continuous momentum spectra were measured for $W \lesssim 2.0$ GeV for the three lowest primary energies at $18^{\circ}$; elsewhere cross sections were measured at intervals in E' of as large as 0.5 GeV. The momentum transfer $Q^2$ ranged from 0.5 $GeV^2$ to 20.0 $GeV^2$ and W ranged as high as 5.2 GeV in this experiment. In this paper the totality of data for either target measured at a constant scattering angle will be called a "triangle", and a

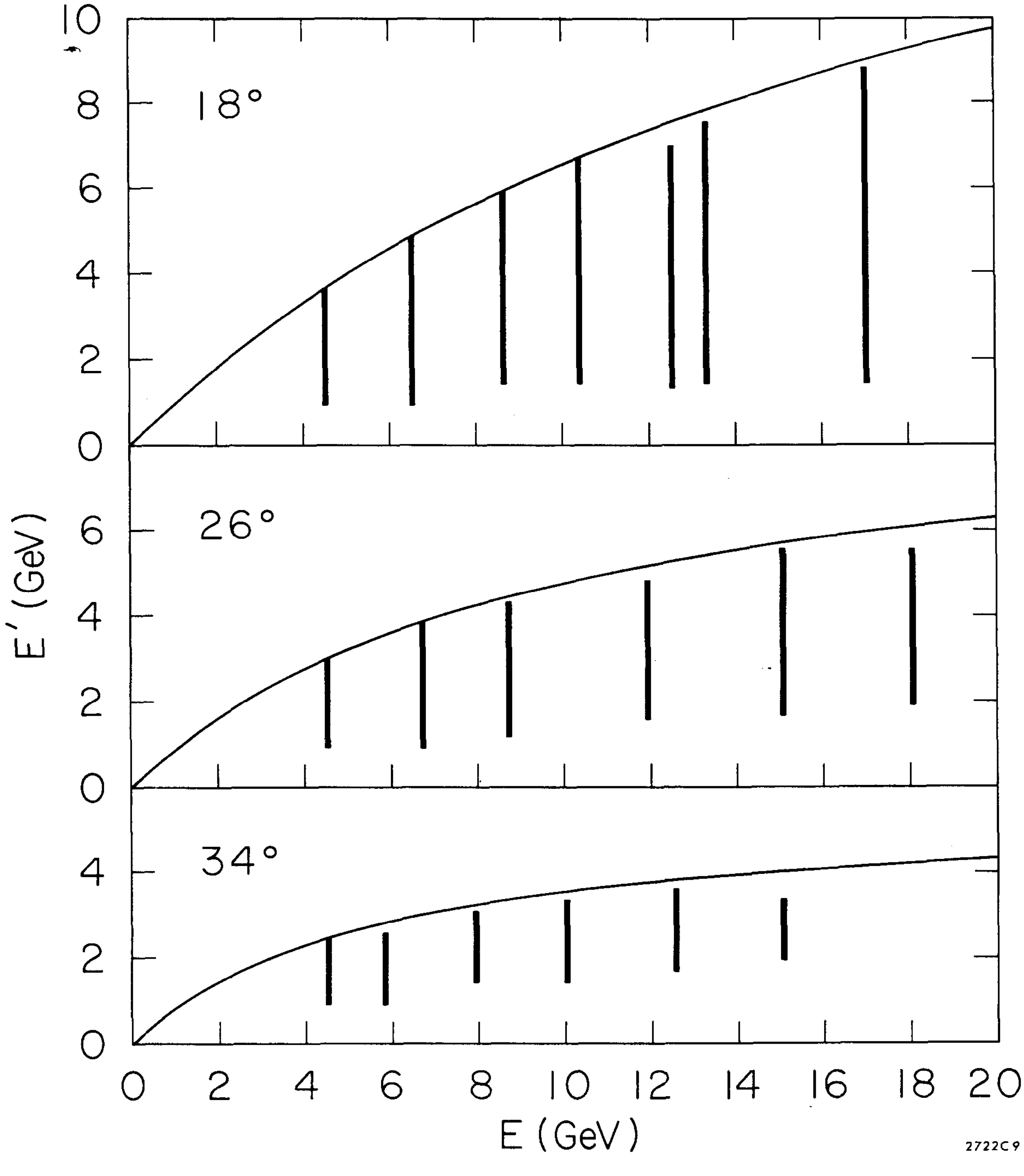


Fig. 2. Ranges of E and E' in experiment A.

single momentum spectrum at fixed primary energy will be called a "line".

In experiment B[25], inelastic e-p and e-d cross sections were measured with the 8 GeV spectrometer at scattering angles of 15, 19, 26, and 34 degrees. Primary energies ranged from 8.7 GeV to 20.0 GeV; the ranges of E' measured at each energy and angle are shown in Figure (3). The momentum transfer $Q^2$ ranged from 4.0 $GeV^2$ to 21.8 $GeV^2$ while W ranged up to 4.1 GeV. This experiment improved the accuracy of the e-p and e-d cross section measurements for $\omega \lesssim 2$ at $26^o$ and $34^o$ and provided entirely new data at $15^o$ and $19^o$. The primary purpose of experiment B was to gain improved accuracy in the measurement of $\sigma_n/\sigma_p$ and of the proton, neutron, and deuteron structure functions in the threshold region ($\omega < 2$).

A diagram of the experimental setup is shown in Figure (4). An essentially monochromatic beam of electrons was focused onto liquid hydrogen and deuterium targets located directly over the spectrometer pivot in End Station A. Two precision toroidal charge monitors were used to measure the incident flux, and several fluorescent screen devices served to monitor the beam steering and focusing. A remotely movable Faraday Cup was periodically inserted into the beam line to calibrate the toroid monitors. The SLAC 1.6 GeV spectrometer, set to detect elastic and quasi-elastic recoil protons, was used to monitor the target densities. Momentum analysis of the scattered particle flux was accomplished

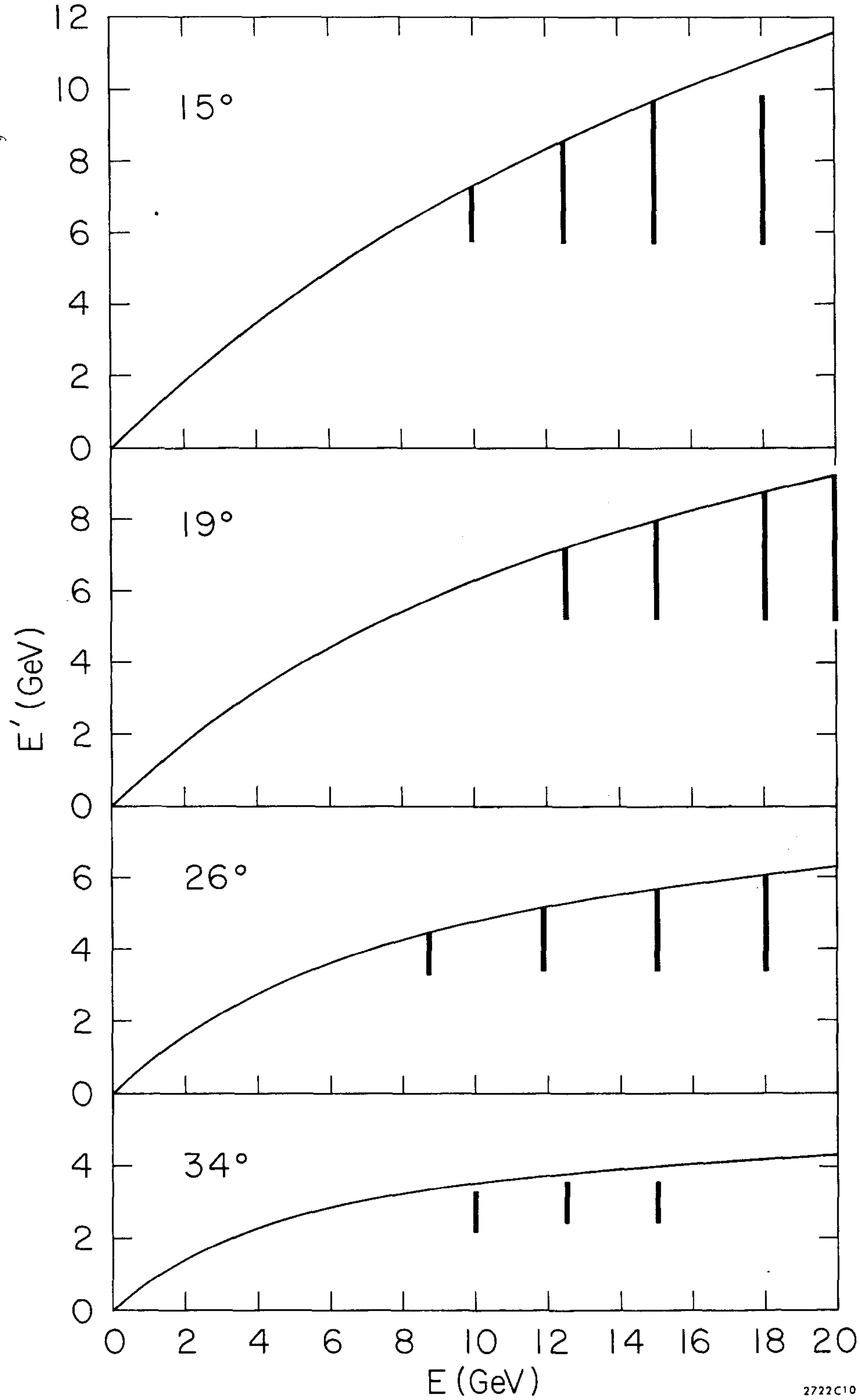


Fig. 3. Ranges of E and E' in experiment B.

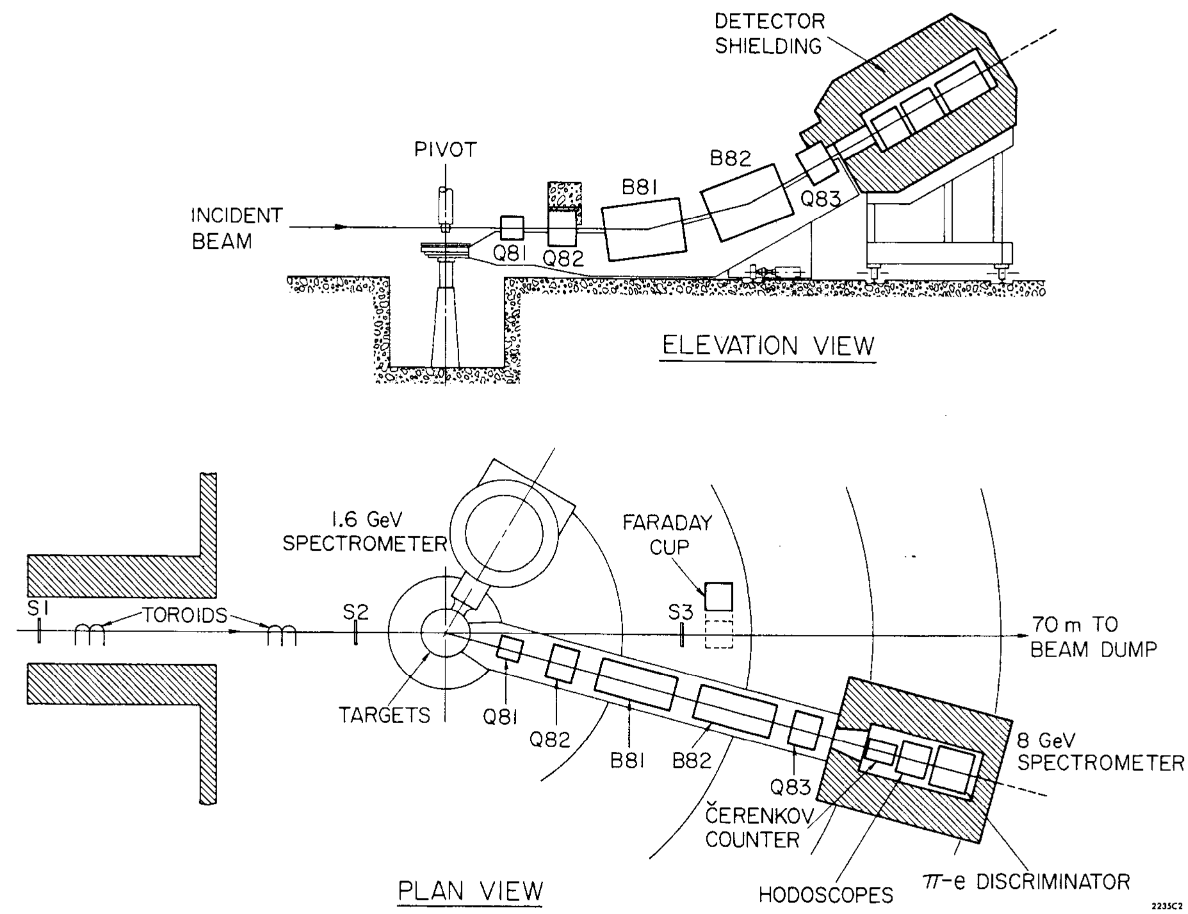


Fig. 4. The experimental set-up.

with the SLAC 8 GeV spectrometer set to the desired scattering angle. The focus of the spectrometer was instrumented with trigger counters for event timing and hodoscopes to determine the angle and momentum of the scattered particles. Separation of electrons from the perdominantly pion background was accomplished with a threshold Cerenkov detector and a $\pi$-e discriminator, which included a multi-layered lead-lucite shower counter and three counters that sampled the early shower development. Signals from the various devices were processed by an on-line SDS 9300 computer, which logged event information from fast electronic logic onto magnetic tape, provided a partial on-line analysis of the data, and monitored the instrumentation during the course of the experiments.

Measured "raw" cross sections were derived from the number of electrons scattered into the spectrometer acceptance for each setting of E, E', and $\theta$. Contributions to the electron yields from the target cell walls were determined using empty replica targets. Measurements with hydrogen, deuterium, and replica targets were interleaved to minimize systematic effects. Contributions from background processes such as $\pi^0$-decay and electron pair production were determined by reversing the spectrometer polarity. Thus the raw cross sections were derived after the contributions from empty target and positrons were subtracted.

Radiative corrections were then applied in two steps to extract the corrected cross sections for inelastic e-p and e-d scattering. In the first step radiative tails from elastic e-p and from elastic and quasi-elastic e-d scattering were subtracted from the raw e-p and e-d cross sections. Inelastic radiative tails were then calculated and subtracted using a model-independent method. The inelastic e-n cross sections were calculated from the corrected e-p and e-d cross sections, using an impulse approximation method which included the effects of Fermi motion of the nucleons in the deuteron.

The two structure functions and R were obtained from these cross section data according to equations (I.1) through (I.5). In order to extend the data to the kinematic region $\omega > 5$, inelastic e-p and e-d cross sections measured with the SLAC 20 GeV spectrometer in an earlier experiment[27, 28] (referred to as experiment C) at scattering angles of 6 and 10 degrees were included in the analysis. Separation of the structure functions and R was then possible over the kinematic region $0.1 \leq x \leq 0.8$, with $1 \leq Q^2 \leq 16\ \mathrm{GeV}^2$ and $1.8 \leq W \leq 5.0$ GeV. The extraction of the structure functions required a careful normalization of these experiments, as all three experiments used different target cells, and experiment C used a different spectrometer. Experiment B was normalized to experiment A by a comparison of the inelastic e-p and e-d cross sections measured at similar E and E' at $26^{\circ}$ and $34^{\circ}$. Experiment C was normalized to experiment A by a comparison of the elastic e-p cross sections measured in the two experiments.

The results reported in this paper are derived primarily from the data of experiments A and B. Whenever significant data have been included from experiment C, this fact will be made clear in the text. As the experimental apparatus and data analysis methods of experiments A and B were nearly identical, we report the two experiments in a single paper. In the following two sections, we describe the experimental apparatus and analysis methods of experiment A. Where these differ from those used in experiment B, additional descriptions are included.